7th IFAC Symposium on Advances in Automotive Control
The International Federation of Automatic Control
September 4-7, 2013. Tokyo, Japan

Design of Fault Tolerant Control System for Electric Vehicles with Steer-by-Wire and In-Wheel Motors

Akira ITO * **Yoshikazu HAYAKAWA** **

* *DENSO CORPORATION, Aichi, JAPAN,*
(e-mail: AKIRA_ITO@denso.co.jp)
** *Graduate School of Engineering, Nagoya University, Aichi, JAPAN,*
(e-mail: hayakawa@nuem.nagoya-u.ac.jp)

Abstract: In this paper we propose a fault tolerant control method which is capable of mitigating steering and drive-train system failures. By utilizing the steering system and the drive-train system complementarily, the proposed method will not need an additional redundancy for the fault tolerant purpose. For the steering system failure which should be detected and managed rapidly, the proposed method utilizes the disturbance observer idea to eliminate the fault detection. On the other hand, for the drive-train system failure, a fault detection is equipped. The effectiveness of this method has been verified in simulation.

Keywords: fault tolerant, disturbance observer, redundancy, steer-by-wire, in-wheel motor

1. INTRODUCTION

The relatively recent development of an electronics technology has given impetus to create a next-generation vehicle. X-by-wire, in particular, has been attracting attention as a technology to dramatically change a today's vehicle. As represented by fly-by-wire for airplanes, X-by-wire is the technology which interprets a driver's intent via sensors and generates electrical commands for actuators. Due to communication by electrical signal, a mechanical linkage is not required. Elimination of the mechanical linkage has brought many significant benefits, such as improvement in fuel consumption, pre-crash safety, crash safety, vehicle architectural flexibility, and so on. Therefore, a replacement of all mechanisms of a vehicle by X-by-wire, such as steer-by-wire, shift-by-wire, and brake-by-wire, has been attempted.

On the other hand, there are many issues with safety if a failure occurs. The difficulty of securing safety prevents X-by-wire products from being popularized. A conventional system, which has secured safety by two or more sensors, microprocessors, and actuators, is very expensive and increases a vehicle's weight, so vehicles equipped with X-by-wire are limited to luxury types. The most important issue of designing X-by-wire products is to secure safety at a suitable cost.

In order to solve these issues, a lot of researchers have already investigated a fault tolerant method of X-by-wire. There are also several significant challenges associated with the fault tolerant of steer-by-wire and drive-by-wire. For instance, combining a steering wheel with a rack axis, switching to a back-up steering motor, and complementing a failure with a rear-wheel steering system have been applied to a steer-by-wire fault tolerant system (Cesiel et al. (2006), Verschuren et al. (2006)). On the other hand, reallocating the driving force lost by a failure to other normal wheels, for a vehicle where all four wheels have independent torque control, has been applied to a drive-by-wire fault tolerant system (Yamaguchi et al. (2006), Wang et al. (2009)). These previous works handle only either a steering or a drive-train system failure. Furthermore, these methods do not take into consideration a cooperation with other systems and attempt to secure safety by sensors, microprocessors, and actuators of one's own. As a result, an additional redundancy for both a steering and a drive-train system is required. Therefore these methods may also have a negative impact on a cost and a vehicle's weight.

Taking into account these issues, we propose a fault tolerant control system for steer-by-wire which requires neither a fault detection nor an additional redundancy for the fault tolerant purpose (Ito et al. (2012)). However our proposed fault tolerant control system is also based on the assumption that the drive-train system does not have any trouble.

In this paper, we propose a more practical fault tolerant control system for mitigating steering and drive-train system failures, which does not require an additional component redundancy for the fault tolerant purpose. In the proposed fault tolerant control system, the steering system failure, which requires a quick corrective action, is immediately compensated for by the drive-train system without a fault detection. On the other hand, the drive-train system failure, which does not require a quick corrective action, is compensated for by the fault detection and the steering system. Finally, we confirmed the effectiveness of the proposed method in the simulation.

2. MODELING

The electric vehicle discussed in this paper is equipped with steer-by-wire and in-wheel motors. The planar dy-

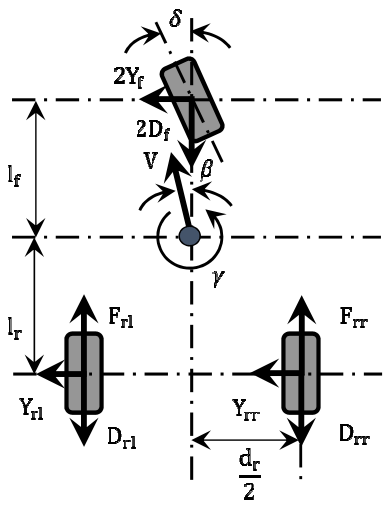

Fig. 1. Vehicle model

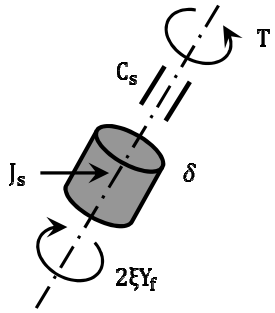

Fig. 2. Steer model

namics of the vehicle are modeled using the three-wheel vehicle model as shown in Fig. 1, where left and right tire forces are affected independently.

$$m\dot{V} = F_{rr} + F_{rl} - D \tag{1}$$

$$mV(\dot{\beta} + \gamma) = 2Y_f + Y_{rr} + Y_{rl} \tag{2}$$

$$J\dot{\gamma} = 2Y_f l_f - (Y_{rr} + Y_{rl})l_r + \frac{d_r}{2}(F_{rr} - F_{rl}) \tag{3}$$

The rolling resistances $2D_f$, D_{rr}, and D_{rl} appear in (1) as a total resistance

$$D = 2D_f + D_{rr} + D_{rl}. \tag{4}$$

The cornering forces Y_f, Y_{rr}, and Y_{rl} have non-linear characteristics given by the following equations:

$$Y_f = -K_f \frac{\tan^{-1}(k_f \alpha_f)}{k_f} \cos(\beta - \delta) \tag{5}$$

$$Y_{rr} = Y_{rl} = -K_r \frac{\tan^{-1}(k_r \alpha_r)}{k_r} \cos\beta \tag{6}$$

where k_f and k_r are a front and rear friction coefficient of a road surface, α_f and α_r are a front and rear slip angle given by

$$\alpha_f = \tan^{-1}\Big(\frac{l_f}{V}\gamma\cos\beta\Big) + \beta - \delta \tag{7}$$

Table 1. Variables

Variable	Symbol
Vehicle slip angle	β
Yaw rate	γ
Vehicle-wheel steering angle	δ
Front tire cornering force	Y_f
Rear left and right tire cornering force	Y_{rl}, Y_{rr}
Steering motor torque	T
Rear left and right tire driving/braking force	F_{rl}, F_{rr}
Front tire rolling resistance	D_f
Rear left and right tire rolling resistance	D_{rl}, D_{rr}
Vehicle speed	V

Table 2. Parameters

Parameter	Symbol
Vehicle mass	m
Moment of vehicle inertia	J
Distance between front tire and center	l_f
Distance between rear tire and center	l_r
Rear tread	d_r
Moment of steering inertia	J_s
Damping coefficient of steering	C_s
Trail	ξ

$$\alpha_r = \tan^{-1}\Big(-\frac{l_r}{V}\gamma\cos\beta\Big) + \beta. \tag{8}$$

The models of cornering forces (5)–(8) are too complicated to use when a fault tolerant controller is considered. Thus, in order to design the controller, the following equations are used

$$Y_f = -K_f(\beta + \frac{l_f}{V}\gamma - \delta) \tag{9}$$

$$Y_{rr} = Y_{rl} = -K_r(\beta - \frac{l_r}{V}\gamma) \tag{10}$$

which are derived by linearly approximating (5)–(8) around the origin of (β, γ, δ). Notice that the linear models (9) and (10) are used for control design, while the nonlinear models (5)–(8) are used for numerical simulations in this paper.

In addition, we consider a steering system (see Fig.2) given by

$$J_s\ddot{\delta} + C_s\dot{\delta} = T - 2\xi Y_f \tag{11}$$

where the steering motor torque T includes the commanded motor current, the motor constant relating current to torque, and the gearbox ratio. The second term $2\xi Y_f$ is the aligning moment resulting from lateral tire forces.

It is easy to imagine that a driver would try to generate not only the yaw rate but also the lateral acceleration in the case of an emergency avoidance maneuver. Thus, a linear combination of the yaw rate γ and the lateral acceleration $V(\dot{\beta} + \gamma)$, i.e.,

$$D^* = dV(\dot{\beta} + \gamma) + (1 - d)V\gamma \quad (0 \le d \le 1) \tag{12}$$

is adopted as the control output (Moriyama (2004)).

Summing up the modeling shown above, the vehicle model for controller design is given by (2), (3), and (9)–(12) with the vehicle speed V being constant, where the control

inputs are T, F_{rr}, and F_{rl}, and the control output is D^*. This model is a linear time-invariant system, so the transfer function model is given by

$$D^*(s) = [\, G_1(s) \;\; G_2(s) \;\; -G_2(s) \,] \begin{bmatrix} T(s) \\ F_{rr}(s) \\ F_{rl}(s) \end{bmatrix}. \qquad (13)$$

Notice that the vehicle model for numerical simulation is given by (1)–(8), (11), and (12), which is a nonlinear system with the vehicle speed V being varying.

3. DESIGN OF FAULT TOLERANT CONTROL SYSTEM

In this paper, we assume a situation in which either the steering system or the drive-train system fails, where a steering system failure means that the steering motor torque is forced to zero ($T = 0$) and a drive-train system failure means that one of two in-wheel motors driving torque is forced to zero ($F_{rr} = 0$ or $F_{rl} = 0$). Notice that the simultaneous failure of the steering system and the drive-train system is not considered.

These failures occur when the driver integrated-circuit (IC) cuts the current due to over-current and over-heating of the motor. The reason why we consider these situation is that the protective function of the driver IC will work first and prevent a permanent failure such as a steering-lock, a self-steering, and a vehicle overrun.

The purpose of the fault tolerant control system proposed in this paper is to prevent unintended vehicle behavior after the failure occurrence and to allow an avoidance maneuver. A block diagram presented in Fig.3 shows a basic structure of the proposed fault tolerant control system. The D^* control block has a role of the fault tolerant for the steering system failure. The force distribution and the fault detection blocks have a role of the fault tolerant for the drive-train system failure. We will explain these functions in detail in the following subsections. The driving force demand block has a role of calculating the driving force command by an accelerator pedal angle. X_+, X_-, and T_c are command signals of the driving force, the left and right driving force difference and the steering motor, respectively.

3.1 D^* Control

We consider a steer-by-wire control system as shown in Fig.4. D^*_{ref} is a target value of the output D^*, which

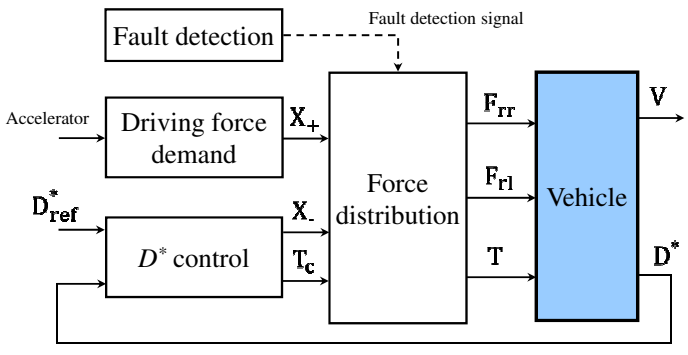

Fig. 3. Fault tolerant control system

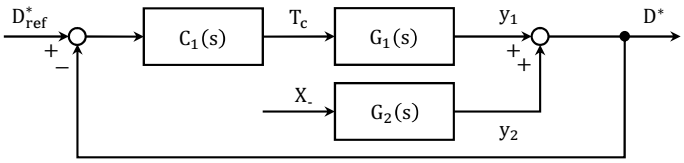

Fig. 4. Steer-by-wire control system

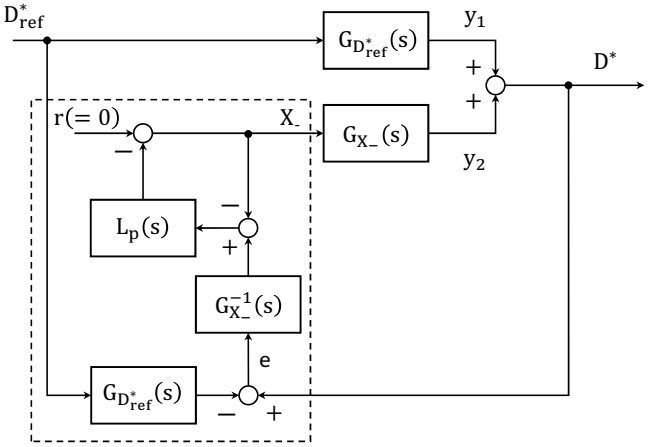

Fig. 5. D^* control block

is calculated from a steering wheel angle or a steering wheel torque. $C_1(s)$ is a steering motor controller, which is derived by applying optimal regulator and Kalman filter design techniques to $G_1(s)$ with an integrator. Notice that a part which distributes X_-, T_c to F_{rr}, F_{rl}, and T is omitted in Fig.4.

It is easy to see from Fig.4 that $D^*(s) = G_{D^*_{ref}}(s)D^*_{ref} + G_{X_-}(s)X_-(s)$ where

$$G_{D^*_{ref}}(s) = \frac{G_1(s)C_1(s)}{1 + G_1(s)C_1(s)} \qquad (14)$$

$$G_{X_-}(s) = \frac{G_2(s)}{1 + G_1(s)C_1(s)}. \qquad (15)$$

The main part of D^* control block is shown as a dotted box (Fig.5) with a low pass filter $L_p(s)$, which corresponds to the disturbance observer.

In fact, in the normal situation, the signal "e" in Fig.5 is zero, i.e., Fig.5 is consistent with Fig.4. On the other hand, when the steering system fails ($T_c = 0$ in Fig.4), the signal y_1 is not controlled and thus the signal "e" becomes nonzero, i.e., the disturbance observer starts working. In this situation, the transfer function $W(s)$ from D^*_{ref} to D^* is derived easily to

$$W(s) = G_{D^*_{ref}}(s). \qquad (16)$$

If the modeling errors are taken into consideration, $G_{D^*_{ref}}(s)$ and $G^{-1}_{X_-}(s)$ in the dotted box (Fig.5) are changed to those models $\hat{G}_{D^*_{ref}}(s)$ and $\hat{G}^{-1}_{X_-}(s)$, respectively. Then the transfer function $W(s)$ turns out to be

$$W(s) = \hat{G}_{D^*_{ref}}(s) \frac{1}{1 + \dfrac{1 - L_p(s)}{L_p(s)} \dfrac{\hat{G}_{X_-}(s)}{G_{X_-}(s)}}, \tag{17}$$

which means that in the low-frequency range (i.e., $L_p(s) \to 1$), $W(s)$ is almost equal to $\hat{G}_{D^*_{ref}}(s)$. Therefore it can be concluded that the steering system failure can be removed almost perfectly by the proposed D^* control block even with the modeling errors.

3.2 Force Distribution

The force distribution design is based on the idea of compensating for the drive-train failure effect by utilizing steer-by-wire and one normal in-wheel motor. On the basis of the fault detection signal from the fault detection block, the force distribution block distributes the commands X_+, X_-, and T_c to the vehicle inputs F_{rr}, F_{rl}, and T not to change the relationship between X_+, X_-, T_c and D^*, V.

Figure 6 indicates a detail structure of the force distribution block. SW i ($i = 1, 2, 3, 4$) denotes a switch controlled by the fault detection block.

In the normal configuration (i.e., the drive-train system is normal), all the switches are connected to the terminal "N" as shown in Fig.6. Then it is easy to see that the distribution law is given by

$$F_{rr}(s) = \frac{1}{2}\{X_+(s) + X_-(s)\} \tag{18}$$

$$F_{rl}(s) = \frac{1}{2}\{X_+(s) - X_-(s)\} \tag{19}$$

$$T(s) = T_c(s). \tag{20}$$

Notice that from Figs.4 and 5,

$$D^*(s) = G_1(s)T_c(s) + G_2(s)X_-(s) \tag{21}$$

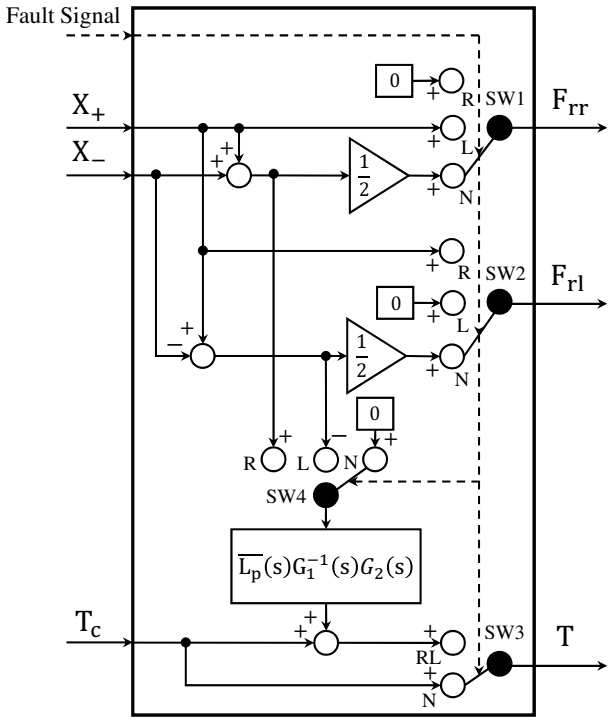

Fig. 6. Force distribution block

where $T_c(s)$ is controlled by the controller $C_1(s)$ and $X_-(s)$ is controlled by the disturbance observer.

When the failure $F_{rr} = 0$ occurs, SW3 is switched to the terminal "RL" and the other switches are changed to the terminal "R" in Fig.6. Then the distribution law is

$$F_{rl}(s) = X_+(s) \tag{22}$$

$$T(s) = T_c(s) + \bar{L}_p(s)G_1^{-1}(s)G_2(s)\{X_+(s) + X_-(s)\} \tag{23}$$

where $\bar{L}_p(s)$ is a low pass filter to make $\bar{L}_p(s)G_1^{-1}(s)$ proper. Note that for the safety, $F_{rr}(s)$ is forced to be zero by SW1. It is easy to see from (1) that (22) allows the vehicle speed V to be invariant. On the other hand, from (13), (22), and (23)

$$\begin{aligned} D^*(s) &= G_1(s)T(s) + G_2(s)F_{rr}(s) - G_2(s)F_{rl}(s) \\ &= G_1(s)T(s) - G_2(s)F_{rl}(s) \\ &= G_1(s)\Big[T_c(s) \\ &\quad + \bar{L}_p(s)G_1^{-1}(s)G_2(s)\{X_+(s) + X_-(s)\}\Big] \\ &\quad - G_2(s)X_+(s) \\ &= G_1(s)T_c(s) + \bar{L}_p(s)G_2(s)X_-(s) \\ &\quad + \{\bar{L}_p(s) - 1\}G_2(s)X_+(s). \end{aligned} \tag{24}$$

Therefore it is concluded that even if $F_{rr} = 0$ happens, in the low-frequency range (i.e., $\bar{L}_p(s) \to 1$) $D^*(s)$ given by (24) is almost same as one given by (21), the normal $D^*(s)$.

When the failure $F_{rl} = 0$ occurs, SW3 is switched to the terminal "RL" and the other swiches are changed to the terminal "L" in Fig.6. Then the distribution law is

$$F_{rr}(s) = X_+(s) \tag{25}$$

$$T(s) = T_c(s) - \bar{L}_p(s)G_1^{-1}(s)G_2(s)\{X_+(s) - X_-(s)\} \tag{26}$$

and the similar argument as in the case of $F_{rr} = 0$ proves that the control object is successfully achieved.

If the modeling errors are taken into consideration, $G_1^{-1}(s)$ and $G_2(s)$ in Fig.6 are changed to those models $\hat{G}_1^{-1}(s)$ and $\hat{G}_2(s)$, respectively. Then (24) turns out to be

$$D^*(s) = \frac{N_D(s)}{D_{DX}(s)} D^*_{ref} + \frac{N_X(s)}{D_{DX}(s)} X_+(s) \tag{27}$$

where

$$\begin{aligned} N_D(s) = & \\ &\Big[\{1 - L_p(s)\}\{1 + \hat{G}_1(s)C_1(s)\}\hat{G}_1^{-1}(s)G_1(s) \\ &+ L_p(s)\bar{L}_p(s)\{1 + \hat{G}_1(s)C_1(s)\}\hat{G}_1^{-1}(s)G_1(s)\Big]\hat{G}_{D^*_{ref}}(s) \end{aligned} \tag{28}$$

$$\begin{aligned} N_X(s) = &\{1 - L_p(s)\} \\ &\{\bar{L}_p(s)G_1(s)\hat{G}_1^{-1}(s)\hat{G}_2(s) - G_2(s)\} \end{aligned} \tag{29}$$

$$\begin{aligned} D_{DX}(s) = &\{1 - L_p(s)\}\{1 + G_1(s)C_1(s)\} \\ &+ L_p(s)\bar{L}_p(s)\{1 + \hat{G}_1(s)C_1(s)\}\hat{G}_1^{-1}(s)G_1(s), \end{aligned} \tag{30}$$

which means that in the low-frequency range (i.e., $L_p(s) \to 1$), (27) is almost equal to $D^*(s) = \hat{G}_{D^*_{ref}}(s) D^*_{ref}$.

4. SIMULATIONS

The proposed method is demonstrated in simulation for a vehicle circling 100[m] in radius at a constant speed of 10 [m/s] for either steering or drive-train system failures. The side slip angle β does not change during a steady circling, then D^* in (12) satisfies the following equation:

$$D^* = V\gamma = \frac{V^2}{R} \tag{31}$$

The target value which realizes a circling 100[m] in radius at a constant speed of 10[m/s] is $D^*_{ref} = 1$. In the simulation, we introduce the nonlinear tire model given by (5)–(8). In addition, vehicle model parameters, i.e., m, J, J_s,C_s,K_f,K_r have a 10% uncertainty of a value in Table 3.

Figures 7–12 show simulation results of the steering system failure. The simulated failure $T = 0$ occurs at $t = 20$[s] as shown in Fig.7. As described in Fig.8, the X_- input increases to compensate for the lack of a circling ability after the failure occurs. Notice that nonzero X_- before $t = 20$[s] is caused for the model parameter uncertainty. Figures 9 and 10 illustrate the vehicle-wheel steering angle δ and the aligning torque $2\xi Y_f$ behavior. From these figures, we can see that the vehicle-wheel steering angle is stabilized in an angle of $2\xi Y_f = 0$ after the steering motor torque $T = 0$. Thanks to the proposed fault tolerant control, the output D^* can track the target value D^*_{ref} and can keep up the circling as illustrated in Figs.11 and 12.

Figures 13–17 show simulation results of the drive-train system failure. The simulated failure $F_{rr} = 0$ occurs at $t = 20$[s] as shown in Fig.13. Notice that the difference between F_{rr} and F_{rl} before $t = 20$[s] is also caused for the model parameter uncertainty. In addition, the drive-train failure is supposed to be detected at $t = 21$[s]. As described in Fig.13, the F_{rl} input increases to compensate for the lack of a driving ability after the fault detection. Furthermore, the steering motor torque also increases to cancel out the effect of yaw moment caused by the biased driving force F_{rl}. Figure 15 shows a vehicle speed. At the moment after the drive-train system failure occurs, the vehicle speed decreases in consequence of rolling resistances. After the fault detection and the driving force reconfiguration, the vehicle can maintain the speed. Thanks to the proposed fault tolerant control, the output D^* can track the target value D^*_{ref} and can keep up the circling as illustrated in Figs.16 and 17.

5. CONCLUSIONS

This paper proposes the fault tolerant control method for the steering or the drive-train system failure. The main feature of this method is that it does not require redundant actuators by taking advantage of existing vehicle functions. We will take into account a possible sensor failure in our future work.

Table 3. Simulation parameters

Symbol	Value	Unit
m	1400	kg
J	2457	kgm^2
l_f	1.02	m
l_r	1.58	m
d_r	1.48	m
J_s	11.98	kgm^2
C_s	9	kgm^2/s
K_f	33700	N/rad
K_r	56200	N/rad
ξ	0.05	m
V	10	m/s

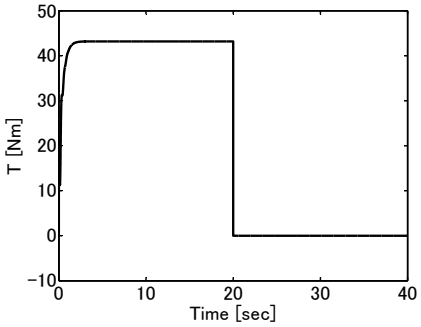

Fig. 7. Steering torque T

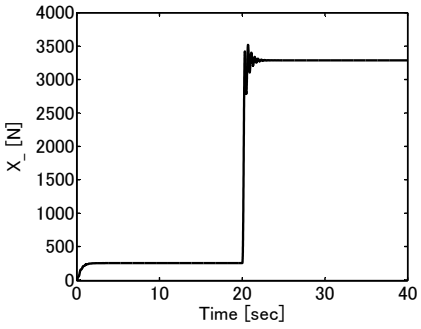

Fig. 8. X_- input

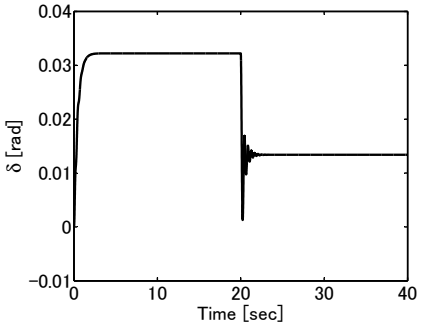

Fig. 9. Vehicle-wheel steering angle δ

REFERENCES

Cesiel, D., Gaunt, M.C. and Daugherty, B. (2006), Development of a Steer-by-Wire System for the GM Sequel, *SAE World Congress*, 2006-01-1173.

Verschuren, R.M.A.F. and Duringhof, H.M. (2006), Design of a Steer-by-Wire Prototype, *SAE World Congress*, 2006-01-1497.

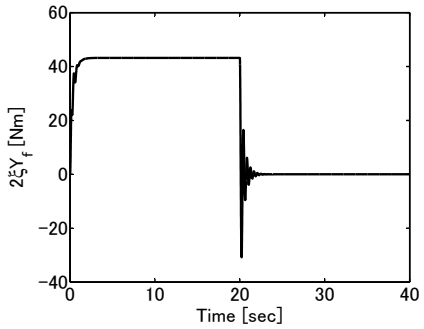

Fig. 10. Self aligning torque $2\xi Y_f$

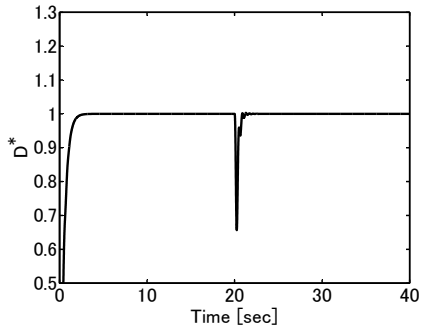

Fig. 11. D^* response

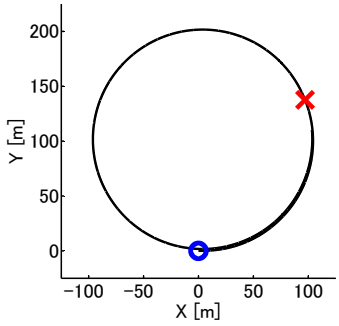

Fig. 12. X-Y plane trajectory (The symbol • indicates the vehicle starting point. The symbol x indicates the simulated failure occurrence point.)

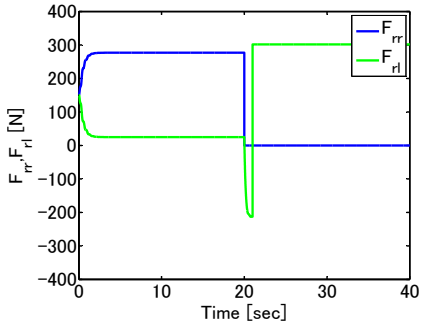

Fig. 13. Driving force F_{rr}, F_{rl}

Yamaguchi, I., Deguchi, Y. and Inoue, H. (2006), Wheel torque distribution reconfiguration for an electric vehicle stabilization: a case study, *International Journal of Automotive Engineering*, 104-06, 11–14 (in Japanese).

Wang, J. and Longoria, R.G. (2009), Coordinated and Reconfigurable Vehicle Dynamics Control, *IEEE Trans. on Control Systems Technology*, 17-3, 723–732.

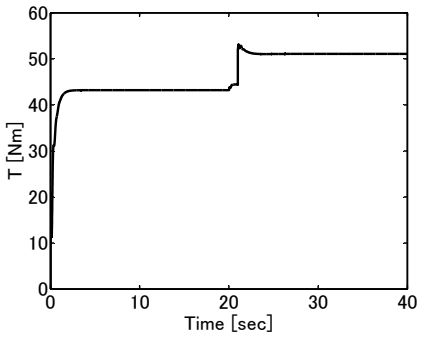

Fig. 14. Steering torque T

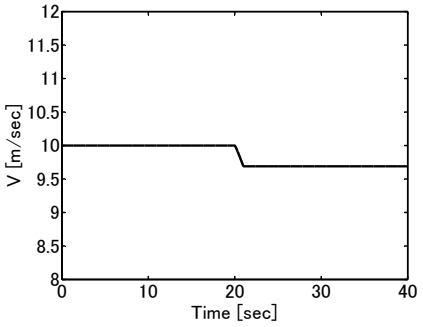

Fig. 15. Vehicle speed V

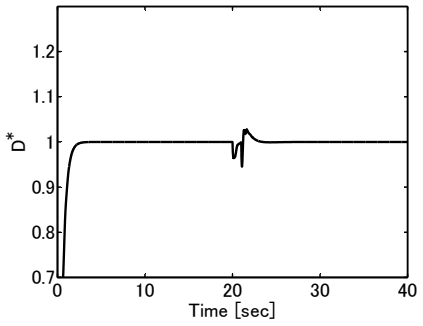

Fig. 16. D^* response

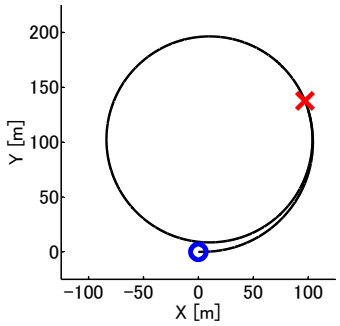

Fig. 17. X-Y plane trajectory (The symbol • indicates the vehicle starting point. The symbol x indicates the simulated failure occurrence point.)

Ito, A. and Hayakawa, Y. (2012), Design of Fault Tolerant Control System for Steer-by-Wire Depending on Drive System, *Trans. of the Society of Instrument and Control Engineers*, 48-12, 872–881 (in Japanese).

Moriyama, M. (2004), Development Trend of Advanced Steering System, *Koyo Engineering Journal English Edition*, No.165E, 8–13.